A tissue mimicking phantom model for applications combining light and ultrasound

A. Ron[a], N. Racheli[a], I. Breskin[a], R. Shechter[*a]
[a]Ornim Medical Ltd, Israel

ABSTRACT

We describe a stable and reproducible liquid tissue mimicking phantom optimized for applications involving both ultrasound and light waves. The phantom has optical and acoustic properties similar to soft biological tissue. The base material is Glycerol. The TiO2 is added to the Glycerol as scattering particles. An absorbing dye is added to obtain desired absorptions in the Near IR range. The phantom's optical absorption was measured by Spatially Resolved Spectroscopy (SRS). In addition, the optical properties were calculated based on the spatial decay of an acousto-optic signal generated in the phantom, and were compared to those obtained with SRS.

Keywords: Tissue, Phantom, Dye, Acousto-optics, NIRS

1. Introduction

Tissue mimicking phantoms serve a variety of applications. They serve as a common method for calibrating optical spectroscopy instrumentation, they are essential for the research stages of new imaging apparatus, and they may be also used for verification and validation of new technologies for monitoring tissue. The requirements from phantoms vary according to the application, where the three major factors are repeatability, reproducibility and stability. Developing and producing phantoms meeting the physical requirements along with these quality requirements is a challenging task.
Whereas many "off the shelf" phantoms for diffused light spectroscopy are offered, it is not straightforward to find a ready-made phantom for applications involving both ultrasound and light. The additional requirements for such a tissue mimicking phantom call for a low acoustic attenuation, an acoustic impedance (acoustic impedance of tissue $1.99*10^6 kg/cm^2 s$) and sound velocity similar to tissue ($1.73 \cdot 10^5 cm/s$) and when coherent properties of light are important to the measurement, the de-correlation time should also be similar to that of the tissue[(1)]. When using the acousto-optic effect to assess the optical properties of the phantom, both the optical properties, the acoustic properties and the de-correlation time should be maintained in order to extract a reliable signal in comparison to live tissue.

Measuring the effective optical attenuation by the acousto-optic effect:
Considering the photon distribution in the presence of a scattering as well as absorbing medium, the underlying assumption that leads to the photon distribution is that the photons are diffusive, i.e. many scattering events occur during the time between absorption events.

When using the acousto-optic effect, ultrasound waves are introduced to a medium containing optical absorbing and scattering centers. The ultrasound (US) wave varies the density of the medium through which it propagates, which in turn leads to changes in the tissue's optical properties, thus forming a modulated scattering pattern for the light. Those photons that scatter of this pattern are called ultrasound modulated (UTL), or 'tagged'.
Following, we describe the extraction of the difference in the optical properties of a uniform medium using the acousto-optic effect:
A coded waveform (GWF) actuates an ultrasound transducer with a known bandwidth, for irradiating the medium with acoustic waves in the form of a non-periodic sequence. Concurrently, coherent light at wavelength λ (generated using laser diodes) is also introduced into the medium. This light propagates through the same volume through which the acoustic waves propagate (tagged volume), and light scattered from the medium is detected by a photodetector with a bandwidth higher than the transducer frequency and bandwidth.

*revital@ornim.com ; www.ornim.com

The detected signals converted to digital signals with an A/D board. The cross correlation between the detected light and the ultrasound waveform GWF is calculated with different time delays τ. For each time delay τ, the amplitude of the cross-correlation *(CCA(τ, λ))* is stored in memory.
Figure 1 shows the amplitude of *C(z, λ)* (i.e. amplitude of cross correlation *CCA(τ, λ)*), obtained for different values of delay τ, as a function of distance from the acoustic transducer, where this distance equals to the product of τ by the speed of sound in the medium (c_s). Three graphs are presented, showing *CCA(τ, λ)* calculated from experimentally obtained signals corresponding to a light response at three different wavelengths $\lambda^1,\lambda^2,\lambda^3$, respectively.

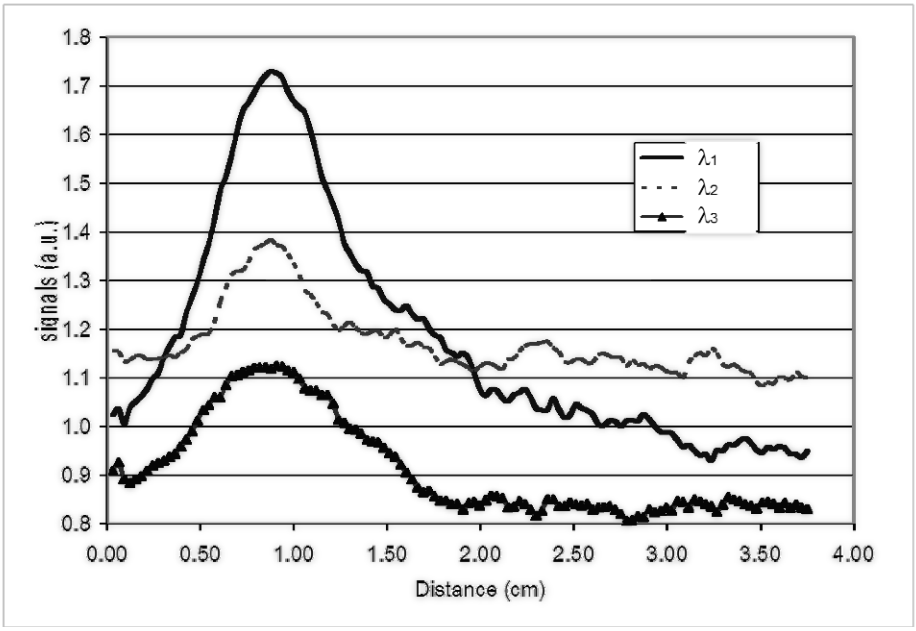

Figure 1. Amplitude of the cross correlation C(z) for three different wavelengths, where $z=c_s * \boldsymbol{\tau}$.

In this example, three different light sources, at three different wavelengths, illuminate a turbid medium, and a detection unit generates electronic signals indicative of measured data corresponding to light collected by the detector, for each wavelength used. As can be seen in the figure, the amplitudes of cross correlation signals *CCA(τ, λ^1)*, *CCA(τ, λ^2)*, *CCA(τ, λ^3)*, or generally *CCA(τ, λ^i)*, at varying distances is different for the three wavelengths. This results from the fact that the light distribution of the three wavelengths in the tissue is different, due to differences in absorption, scattering and index of refraction.
The correlation *CCA(τ, λ^i)* corresponds to the acoustic distribution or pressure amplitude *PA(z)*, and to the light distribution [(2)] *LD(λ^i)*.

$$LD(z,\lambda^i) = K * \prod_{\alpha=s,d}\left(1+\frac{1}{\mu_e^i\sqrt{(\vec{r}-\vec{r}_\alpha)^2+z^2}}\right)\frac{z}{(\vec{r}-\vec{r}_\alpha)^2+z^2}\exp\left(-\mu_e^i\sqrt{(\vec{r}-\vec{r}_\alpha)^2+z^2}\right) \quad [1]$$

where *K* is a constant, $\mu_e^i = \sqrt{3\mu_a^i\left(\mu_a^i+\mu_s^i\right)}$ is the effective decay rate of light in the medium, μ_a^i is the absorption coefficient and μ_s^i is the scattering coefficient at wavelength λ^i ; when near infrared light is used, it can be assumed that $\mu_a^i << \mu_s^i$ and thus $\mu_e^i \cong \sqrt{3\mu_a^i\mu_s^{\,i}}$, $\vec{r}_\alpha$ is either the vector to the source ($\alpha = s$) or to the detector ($\alpha = d$), and z is the direction parallel to the direction of propagation of the acoustic radiation into the medium.
For example, for a large enough distance *z* ($z= \tau \cdot c_s$) from the body surface (namely larger than the mean free path of light in the medium, and larger than the source detector separation, $\vec{r}_d - \vec{r}_s$, the light distribution *LD(z,λ^i)* is proportional to

$e^{-2\mu^i z}$, where *CCA(z,λ^i))* is given by $CCA(z,\lambda^i) \cong PA(z) I_0^i e^{-2\mu^i z} + C_o$, where I_0^i is the initial light intensity upon entry into the medium, PA is the acoustic pressure and C_o is an additive constant.
Thus, if the acoustic pressure amplitude *PA(z)* is known, for example by measuring it with a hydrophone in water, the light distribution *LD(z,λ^i)* can be extracted by dividing *PA(z)* out of *CCA(z ,λ^i)*, after eliminating C_o. In many practical cases, however, the pressure profile is unknown, for example when the medium consists of different layers with different acoustic impedances. Thus, there may be no correspondence between measurements of the pressure profile in water or synthetic phantoms and the actual pressure profile in the measured medium. In such cases, measurements with at least two or generally *N* different light wavelengths can be performed, and corresponding *CCA(z,λ^i)* are used to eliminate the acoustic contribution *PA(z)* (after eliminating C_o). This is implemented by dividing measured *CCA(z,λ^i)* by measured *CCA(z,λ^j)* for *i≠j*, assuming that the acoustic contribution is the same for all optical wavelengths. Thus, the ratio of the light distributions can be obtained. This ratio is important for example for determining the oxygen saturation of blood in tissue.
In the case of a medium irradiated by three different wavelengths:

$$\frac{\tilde{I}^i}{\tilde{I}^j} = \frac{I_0^i}{I_0^j} e^{-2\Delta\mu_e^{ij} z} \qquad [2]$$

where *i; j* = 1*;* 2*;* 3 represent the three lasers, $\tilde{I}^i = \left(CCA(z,\lambda^i) - C_o\right)$ is the amplitude of the signal at distance z, I_0^i, I_0^j are the input intensities of the ith and jth wavelengths respectively and $\Delta\mu_e^{ij} = \mu_e^i - \mu_e^j$. The constant C_o corresponds to the noise level of the system at the measured frequency bandwidth. For example, one possible way to measure C_o, is to cross correlate the measured signals with a time-reversed signal $S_p(\tau\text{-}t)$. Such a correlation results in the same frequency bandwidth, but is completely uncorrelated the signals. Thus, constant C_o for each wavelength of light can be measured independently and eliminated from signal *CCA(z,λ^i)*.
Taking a logarithm of the equation above, $\Delta\mu_e^{ij}$ can be obtained

$$\Delta\mu_e^{ij} = -\frac{1}{2}\frac{\partial}{\partial z}\ln\left[\frac{\tilde{I}^i}{\tilde{I}^j}\right] \qquad [3]$$

Measuring the effective optical attenuation using SRS:

The effective attenuation coefficient μ_e was measured by the method of "spatially resolved spectroscopy". This method derives μ_e from, the diffuse reflectance as a function of the distance r_{sd} between the source and the detector for a semi-infinite half-space geometry[2]. Figure 2 shows schematically the "banana" of photons propagating between source and detector, symbolizing the statistical majority of paths travelled by photons reaching the detector.

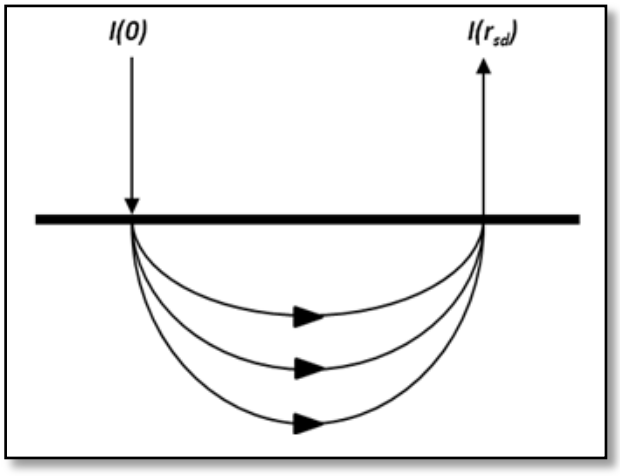

Figure 2 The photons paths in a semi-infinite medium

As discussed above, when $\mu_s >> \mu_a$ the effective attenuation coefficient is reduced to $\mu_e = \sqrt{3\mu_a\mu_s'}$.,
The reflectance is given by [2]:

$$R(r_{sd}) = \frac{1}{\mu_s}\frac{e^{-\mu_e r_{sd}}}{2\pi r_{sd}^2}\left(\mu_e + \frac{1}{r_{sd}}\right)$$

The effective attenuation coefficient is derived by multiplying both sides by r_{sd}^2 and taking the logarithm:

$$\ln\left(r_{sd}^{\,2} \cdot R(r_{sd})\right) = -\mu_e \cdot r_{sd} + \ln(\mu_e + \frac{1}{r_{sd}}) + const$$

For $r_{sd} >> 1/\mu_e$, plotting $\ln\left(r_{sd}^{\,2} \cdot R(r_{sd})\right)$ as a function of r_{sd}, provides μ_e.
In our experimental setup, the distance between transmission and detection (r_{sd}) was gradually changed from 18 to 25mm and the intensity $R(r_{sd})$ was measured using a fiber connected to a power meter

2. Methods

Phantom Preparation

The Phantom comprises of Glycerin 99% (Sigma Aldrich) into which TiO2 (Sigma Aldrich) was added at a concentration of 0.1% by weight as scattering particles. ProJet-800NP (Fujifilm) at different concentrations of 0.0003% to 0.0009% by weight and diluted in 1-Methoxy-2-Propanol, 99% (Sigma Aldrich) was use as absorber. The mixture was poured into a black plastic container. The container absorbing walls and size (14 X 9.5 X 7.5 cm^3) were chosen for minimizing boundary effects.
The speed of sound in Glycerin equals $1.9\cdot10^5$cm/s. The acoustic impedance equals $2.34*10^6$kg/cm^2s.
ProJet 800NP dye – The ProJet dye by Fujifilm[3] is a Phthalocyanine Infrared Absorber with a distinctive spectral profile and sharp absorption maximum at 775nm. It has a sharp descent in absorbance between 770 and 850nm.

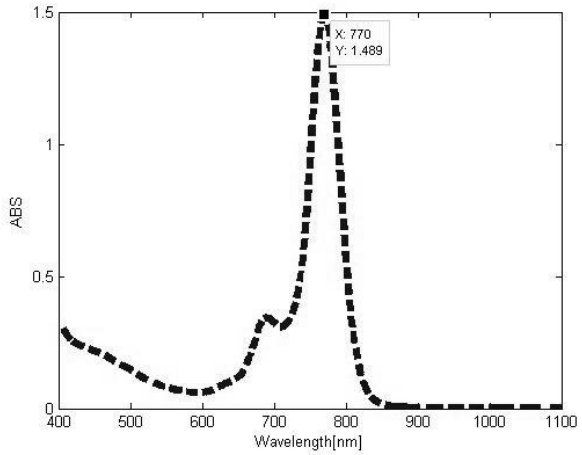

Figure 3 The absorbance curve of ProJet 800NP dye [3].

Measurement of the scattering coefficient μ_s

The scattering coefficient μ_s was measured independently using the collimated transmission method[5] for a mixture containing glycerol and TiO2 in a cuvette and was found to be: μ_s =25.5cm^{-1}. The anisotropy factor g for TiO2 is[4] estimated to be 0.55 at the relevant wavelengths, providing a reduced scattering coefficient of $\mu_s' = \mu_{s*}(1-g)$= 11.48cm^{-1}.

Measurement of the effective attenuation coefficient μ_e using SRS

The phantom's effective attenuation coefficient was measured by the method of "spatially resolved spectroscopy". Three fiber-coupled laser diodes (Innovative Photonic Solutions) at the wavelength of 785, 808 and 830nm were used. Light was delivered to the phantom through a 62.5µ fiber which was immersed into the phantom. A second fiber positioned on a translation stage and also immersed in the phantom was used to collect light at various distances.

The reflectance was measured at the distances between 15mm to 25mm.

Measurement of the effective attenuation coefficient μ_e using Acousto-optics

A schematic diagram of the experimental set-up is presented in Figure 3. An ultrasound transducer was used to generate acoustic waves. A light beam was delivered to the phantom through an optical fiber (62.5µm, NA 0.27), passing through a hole in the transducer's center. A second optical fiber (bundle of 12*200µm, NA=0.22) was used to collect the scattered light and deliver it to a photo-detector (Hamamatsu, C5460-103(x1))

The distance between the light transmission and collection was 11mm.

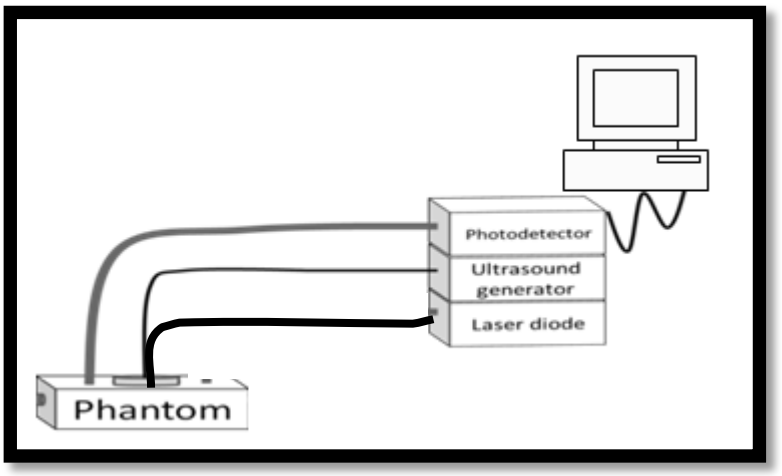

Figure 3 Illustration of the acousto-optic setup

The US sequence (GWF) was generated using a computer controlled function generator. The diameter of the acoustic beam at the surface was 11mm, and the central ultrasound frequency was 1MHz. The photo detector's signals were sampled with an A/D converter. The analysis of the data was performed using MATLAB software.

3. Results

Scattering coefficient

The scattering coefficients (μ_s) were measured using the collimated beam method. It was measured for the three relevant wavelengths 785, 808 and 830$_{nm}$ (λ_1, λ_2 and λ_3 respectively) at different concentrations of TiO_2.

Table 1 Results of µ_smeasurements for TiO2

	0.01% TiO_2 $[cm^{-1}]$	0.02% TiO_2 $[cm^{-1}]$	0.05% TiO_2 $[cm^{-1}]$
λ_1 =785nm	2.6355	5.7149	13.3012
λ_2 =808nm	2.5903	5.4654	12.4437
λ_3=830nm	2.1542	4.9825	12.1779

Effective attenuation coefficient

Phantoms with different ProJet 800NP concentrations were prepared. A larger range of concentrations was measured using the SRS method then by the Acusto-optic (UTL) method due to lower SNR in the latter. The differences in μ_e for $\Delta\mu_e^{\lambda 1-\lambda 2}$ and $\Delta\mu_e^{\lambda 2-\lambda 3}$ measured separately using SRS and Acousto-optics are presented below.

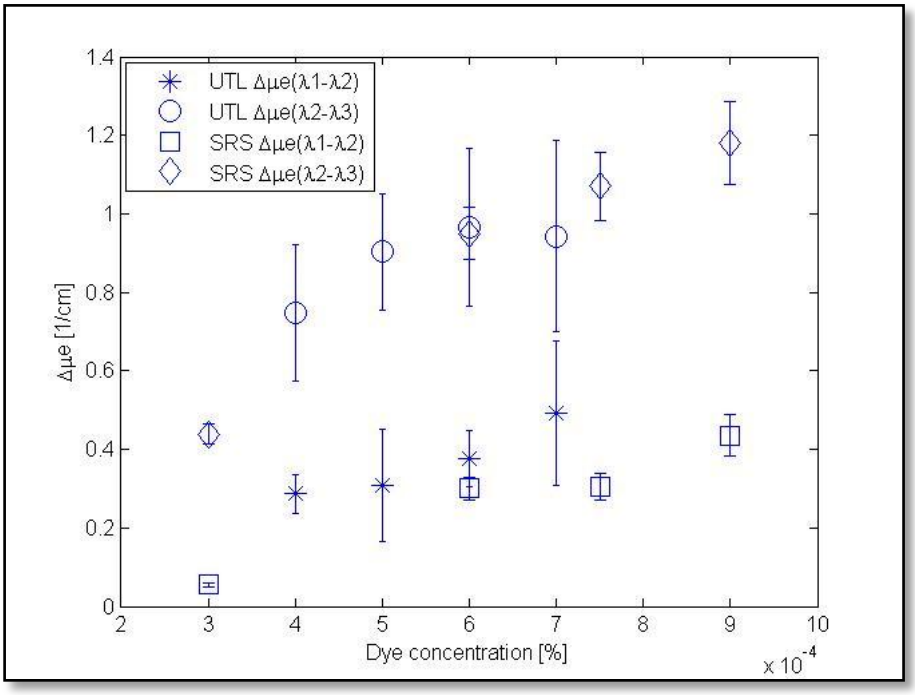

Figure 4 The differences in $\mu_{e,}$ measured by the methods of SRS and UTL. Each method was measured at four different dye concentrations.

Stability

The phantom's stability is demonstrated in figure 5. The intensity of the collected light for each of the three wavelengths is plotted for a nine hour period.

The ratio between the standard deviation to the mean value for λ_{785}, λ_{808} and λ_{830} is 0.64%, 1.25% and 1.07% respectively.

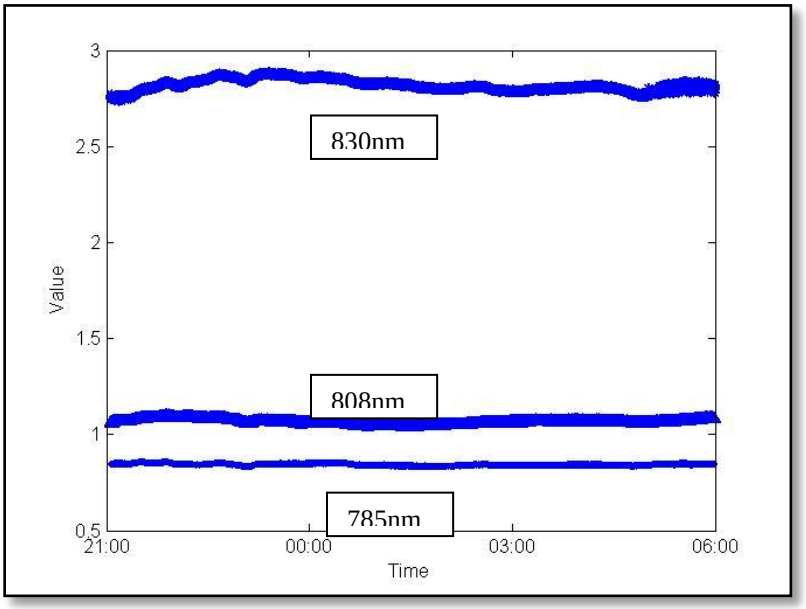

Figure 5 The light amplitude as a funtion of time for the three wavelengths.

4. Discussion

Measurements of the effective attenuation coefficient (μ) or absorption coefficient (μ_a) are essential for extracting Hemoglobin concentration in blood or the ratio of oxygenated to total hemoglobin concentration as in the case of extracting oxygen saturation of hemoglobin. The range of wavelengths around the isosbestic point of oxygenated and de-oxygenated Hemoglobin is usually chosen around 700nm to 850nm.
The suggested Pro Jet 800NP phantom was found effective for estimating the feasibility of an Acousto-optic system to observe the differences in μ_e^i for the relevant wavelength range.

The differences in μ measured between the three wavelengths- 785nm, 808nm and 830nm were significant using both methods, UTL and SRS. Furthermore, both methods produced similar values.
Both methods for measuring μ_e, SRS and UTL, produce a linear increase in $\Delta\mu_e$ as a function of increasing dye's concentration. The differences in the slopes between the two methods could be explained by the fact that the assumptions for calculating μ_e using the Spatially Resolved Spectroscopy method are not fully met in this setting. Due to technical limitations, the transmission-detection separation (r_{sd}) was limited to a certain distance of ~2.5cm. Where the assumption of this method is that $r_{sd} \gg \frac{1}{\mu_e}$, where $\mu_e \approx 1cm^{-1}$. In order to enable a larger r_{sd}, a phantom of larger volume should be use along with stronger emitting power lasers or amplified detectors.
The phantom was shown to be stable during the measurement. In fact, fluctuations of the emitted laser's power are the major cause for the minor variations in the detected light amplitude.

It should be noted that the absorption profile measured was different from the one provided by the manufacturer. This could results from the different solvent used. The expected ratio between differences in absorbance (as supplied by the manufacturer)- $\frac{A_{\lambda 785} - A_{\lambda 808}}{A_{\lambda 808} - A_{\lambda 830}}$ equals 3.41(where A is absorbance) while it is clear from both methods that this ratio was inversed. This inversion can be explained by a shift of the absorbance curve to the left due to the dye dissolving properties.
The effect of shift in the scattering coefficient μ_s as a function of wavelength was previously investigated[4] And was reconfirmed here. It is not used here for the measure of μ_e nevertheless it is necessary for extracting the absorbance coefficients for a future investigation.

REFERENCES

[1] Lev, A., Sfez, B., "In vivo demonstration of the ultrasound-modulated light technique", J. Opt. Soc., 2347-2354 (2003).
[2] Tuchin, V., [Handbook of optical Biomedical Diagnostics], SPIE PRESS, Bellingham, 460, 502-305 (2002).
[3] <http://www.fujifilm.eu/fileadmin/products/Imaging_Colorants/Data_Sheets/Infrared_Absorbers_Sep._2011/Pro-Jet_800NP.PDF>
[4] Firbank, M., Delpy, D. T., "A design for a stable and reproducible phantom for use in near infra-red imaging and spectroscopy." *Physics in medicine and biology* 38.6 (1999).
[5] Firbank, M. "The design, calibration and usage of a solid scattering and absorbing phantom for near infra red spectroscopy" *Doctoral dissertation, University of London* (1994).
[6] AZHARI, H., [Basics of biomedical ultrasound for engineers], John Wiley & Sons, 313 (2009).